Dear Editor and Referees:

We are particularly grateful for your careful reading, and for giving us many constructive comments on this work. According to the comments and suggestions, we have tried our best to improve the previous manuscript ESSD-2022-142 (An improved global land cover mapping in 2015 with 30 m resolution (GLC-2015) based on a multi-source product fusion approach). We believe the revised manuscript accounts for all reviewers' comments, and it was significantly improved as a result. The modified words or sentences are marked as blue color in the revised manuscript. We are providing an item-by-item response to all questions and recommendations.

Thanks very much for your time.

Best regards,

Xiaoping Liu and all co-authors

Reviewer #1:

General comment:

The authors seek to generate a new global LC map by fusing the existing ones using Dempster Shafer theory of evidence. The manuscript is easy to follow and language is always understandable. The technique is routine and lack of innovations. By examining their result, I accidently found an error which suggests the data and method they used may not robust (see my comments below). The new map achieves higher accuracy but also shares the common problems in the existing data, such as unstable performance for specific LCs or in certain areas. As such, I am not convinced that this dataset and manuscript could be candidates for ESSD.

Response**:** Thanks for the comment. These comments are very helpful for revising and improving our paper. The manuscript has been improved according to your and another reviewer's comments. The point-by-point responses are listed below in **blue**. The changes in our manuscript are marked with red.

Although some studies have adopted the Dempster-Shafer theory of evidence to create a hybrid map (Ran et al., 2012; Huang et al., 2022), they focused only on the regional scale. There are a lot of challenges to overcome when applying DSET to land cover mapping at the global scale. First, large and reliable samples are required to evaluate the reliability of the input GLC maps. Visual interpretation of a large number of samples over the globe is labor-intensive and time-consuming. Second, the application of the DSET on a global scale is restricted. Given that the characterization of the land cover landscape varies around the world, the study area must be split into sub-regions so that the quality of the existing GLC maps can be more accurately assessed for different regions. Compared to a single fusion model for regional land cover mapping, a local adaptive fusion model is demanded for global land cover mapping. Third, the traditional local computer processing method is not effective in global land cover mapping due to the lack of high computation resource and the difficulties in preparing image mosaics (Zhang et al., 2021).

To deal with the above problems, we implemented the GLC mapping using following strategies: (1) We used the interpretation-based method to generate a total of 200,000 point-based samples over the world's terrestrial area and used 80% of the samples to evaluate the reliability of each candidate map; (2) The global land was divided into 1507 4°×4° geographical grids, and the accuracy assessment on each product was performed in each grid using local samples. Meanwhile, the corresponding local adaptive fusion method based on the DSET was applied; (3) We implemented the whole LC mapping task on Google Earth Engine platform. With the help of GEE, the computer memory and image processing problems can be solved. In general, our GLC-2015 map is the first 30m-resolution land cover map that successfully overcomes the aforementioned issues in applying the DSET method on a global scale.

Based on the DSET method, the GLC-2015 map obtained better performance than any of the existing ones with an OA improvement of 12.5%-14.7% based on point-based samples and 10.9%-18.5% based on patch-based samples. Especially, our map showed the most substantial outperformance in the areas of high inconsistency, with an accuracy improvement of 21.0%-25.2% compared to 0.2%-1% for areas of low inconsistency and 17.6%-23.2% for areas of moderate inconsistency. In other words, the superiority of our map over other products is more evident in areas with more disagreements (the details can be found in our response to Comment #1-6 and Comment #1-8).

Although the GLC-2015 map provided relatively lower accuracy for grassland, shrubland, and wetland,

its accuracy for these LC classes was higher than the existing products with the PA and OA ranking first or second (the details can be found in our response for Comment #1-8).

Therefore, although there are some classification errors for some specific LC classes and regions, the GLC-2015 product can still provide a more accurate characterization of land cover than the current products and is a good complement to the existing GLC data.

References:

Huang, A., Shen, R., Li, Y., Han, H., Di, W., and Hagan, D. F.: A methodology to generate integrated land cover data for land surface model by improving Dempster-Shafer theory, Remote Sen., 14, 972, https://10.3390/rs14040972, 2022.

Ran, Y., Li, X., Lu, L., and Li, Z.: Large-scale land cover mapping with the integration of multi-source information based on the Dempster–Shafer theory, Int. J. Geogr. Inf. Sci., 26,169-191, https://doi.org/10.1080/13658816.2011.577745, 2012.

Comment #1-1. The GlobeLand30 in 2010 has a 5-year temporal gap between the other datasets. The LC changes in this 5 five years will bias you result. How did you deal with it? Please clarify this in the manuscript.

Response: Thanks for the comment. In the process of fusing the Globeland30, FROM_GLC and GLC_FCS30 for a new map, we just neglected the 5-year interval between the input products. The reasons why we used the Globeland30 and regarded it as reasonable are as follows:

(1) In many existing studies focusing on generating a hybrid map, multisource land cover products with different data times were used (Jung et al., 2006; Xu et al., 2014; See et al., 2015; Song et al., 2017; Tsendbazar et al., 2017). As demonstrated in previous work, the uncertainties from land cover changes are relatively more minor than that from inaccurate classification (Xu et al., 2014). In addition, the LC changes caused by the five-year gap is tiny when it comes to the LC mapping at the global scale. Thus, most spatial disagreements between the existing maps are not about LC changes over the time interval but about classification error and the integration of the maps is aimed at finding the most representative LC class (McCallum et al., 2006; See et al., 2015).

(2) When we implemented the multi-source product fusion based on the DSET method, we used a global point-based sample set verified by manual interpretation for the year 2015 to evaluate the reliability of each GLC product for each LC class in a 4° × 4° grid. If there are land cover changes in some areas from a candidate map due to the time interval from 2015, the reliability of this map is lower based on the assessment with the point-based samples. Thus, the LC classes assigned to the output map will be more likely to come from other input maps.

(3) To improve the performance of a synergetic land cover map, it is better to employ more available products with high quality (Zhong et al., 2019). The Globeland30 product has great popularity due to its good accuracy and worldwide coverage. Also, its classification scheme is almost the same as our target map (GLC-2015).

Given the considerations above, it is reasonable to use the Globeland30 product as one of the input maps though there is a 5-year temporal gap between GlobeLand30 and the two other GLC products

(FROM_GLC and GLC_FCS30).

The content on how we dealt with a 5-year temporal gap between Gloeland30 and other products had been added in our manuscript.

"Although the data time of GlobeLand30 is 2010, which has a five-year gap with other products, it was used in our project for the following reasons: (1) The changed areas of LC caused by the time interval are tiny compared to the global land area. In addition, there is relatively less uncertainty due to LC changes than due to inaccurate classification (Xu et al., 2014). Most spatial disagreements between the existing maps are about classification errors rather than LC changes over the time interval (McCallum et al., 2006; See et al., 2015); (2) We used a global point-based sample set for the year 2015 to evaluate the reliability of the input products in all 4° × 4° grids. At locations where land cover changed between 2010 and 2015, the Globeland30 was more likely to have low accuracy based on the validation and less likely to contribute to the fusion using the DSET approach. In this way, the errors due to land cover changes can be largely avoided; (3) The GlobeLand30 has great popularity due to its good accuracy. The classification system of the GlobeLand30 is almost the same as that in our study." (Revised manuscript, Line 150-160)

Furthermore, we have added the discussion about uncertainties brought by the GlobeLand30:

"Second, the date time of the GlobeLand30 is different from that of other maps. Because of the five-year time interval, there are changes in land cover, which inevitably distort the fusion results. However, the changed areas are tiny compared to the world's terrestrial area. The uncertainties caused by the LC changes are minor than those from classification errors. In addition, the global point-based samples were used to evaluate the reliability of each product. The accuracy of GlobeLand30 was lower than the other products for areas with LC changes. In this case, the fusion depended more on other maps to avoid the errors caused by LC changes." (Revised manuscript, Line 751-757)

References:

Jung, M., Henkel, K., Herold, M., and Churkina, G.: Exploiting synergies of global land cover products for carbon cycle modeling, Remote Sens. Environ., 101, 534-553, https://doi.org/10.1016/j.rse.2006.01.020, 2006.

McCallum, I., Obersteiner, M., Nilsson, S., and Shvidenko, A.: A spatial comparison of four satellite derived 1 km global land cover datasets, Int. J. Appl. Earth Obs. Geoinf., 8, 246–255, https://doi.org/10.1016/j.jag.2005.12.002, 2006.

See, L., Schepaschenko, D., Lesiv, M., McCallum, I., Fritz, S., Comber, A., Perger, C., Schill, C., Zhao, Y., Maus, V., Siraj, M. A., Albrecht, F., Cipriani, A., Vakolyuk, M. y., Garcia, A., Rabia, A. H., Singha, K., Marcarini, A. A., Kattenborn, T., Hazarika, R., Schepaschenko, M., van der Velde, M., Kraxner, F., and Obersteiner, M.: Building a hybrid land cover map with crowdsourcing and geographically weighted regression, ISPRS J. Photogramm. Remote Sens., 103, 48-56, https://doi.org/10.1016/j.isprsjprs.2014.06.016, 2015.

Song, X., Huang, C., and Townshend, J. R.: Improving global land cover characterization through data fusion, Geo-Spat. Inf. Sci., 20, 141-150, https://doi.org/10.1080/10095020.2017.1323522, 2017.

Xu, G., Zhang, H., Chen, B., Zhang, H., Yan, J., Chen, J., Che, M., Li, X., and Dong, X.: A Bayesian based method to generate a synergetic land-cover map from existing land-cover products., Remote

Sen., 6, 5589-5613, https://doi.org/10.3390/rs6065589, 2014.

Tsendbazar, N. E., Bruin, S., and Herold, M.: Integrating global land cover datasets for deriving user-specific maps, Int. J. Digit. Earth., 10, 219-237, http://dx.doi.org/10.1080/17538947.2016.1217942, 2017.

Zhong, Y., Luo, C., Hu, X., Wei, L., Wang, X., and Jin, S. Cropland product fusion method based on the overall consistency difference: A case study of China, Remote Sens., 11, 1065, https://doi:10.3390/rs11091065, 2019.

Comment #1-2. To my knowledge, the GSW data has multiply layers and its historical data is provided monthly. Therefore, how did you derive the water bodies from GSW for 2015. This should be explicitly clarified in the manuscript.

Response: Thanks for the comment. On the GEE platform, the JRC GSW datasets are available with multi subsets as 'Surface Water Mapping Layers', 'Monthly Water History', 'Monthly Water Recurrence', and 'Yearly Water Classification History', so that users can choose them appropriately. For our purpose, we used the GSW Yearly Water Classification History v1.1 in the GEE catalog, which provides the annual dynamics of water presence for the period of 1984 to 2019 at a 30m pixel basis. Each image of this data has a single 'waterClass' band which describes the seasonality of water throughout the year by four different types: no data, no water, seasonal water, and permanent water. Given that the seasonal water in the GSW data is not as reliable as the permanent water (Meyer et al., 2020) and might contain wetland around rivers, lakes, and ponds, we selected GSW data for the year 2015 and the permanent water was regarded as water bodies, while the seasonal water was excluded.

Correspondingly, we have added the clarification of the use of GSW in our manuscript.

"We used the GSW Yearly Water Classification History v1.1 in the GEE catalog. A single 'waterClass' band is present in each image that provides the water's seasonality throughout the year with four types: no data, no water, seasonal water, and permanent water. Since the seasonal water in GSW data is not as reliable as the permanent water (Meyer et al., 2020), we selected permanent water bodies and excluded seasonal water bodies." (Revised manuscript, Line 190-194)

References:

Meyer, M. F., Labou, S. G., Cramer, A. N., Brousil, M. R., and Luff, B. T.: The global lake area, climate, and population dataset, Sci. Data, 7, 174, https://doi.org/10.1038/s41597-020-0517-4, 2020.

Comment #1-3. For single-class datasets (e.g., GSW), how did you deal with the background? Did you just ignore it or treat it as non-water? I think the latter is more useful.

Response: Thanks for the comment. For those single-class datasets, we treated it as another land cover type. If the background information is regarded as a land cover type, these products provide the presence of land cover with two types. For example, the GSW contains "water" and "non-water". In this way, the quality of the GSW can be comprehensively estimated since we can provide the PA and UA for both water and non-water. In our study, "non-water" can be any of other nine class except "water". The PA and UA for the "non-water" were defaulted to 0 since the GSW did not provide information about the other nine LC classes.

In addition, the part has been added as:

"The background information of these single-class products was considered as another land cover class (e.g., non-water) participating in the fusion. The accuracy of the background information was defaulted to 0 since it did not provide information about any of the other nine categories in our classification system." (Revised manuscript, Line 170-173)

Comment #1-4. Why different number of blocks were chosen for patch-based samples while the number of pixel-based samples seems to follow an equal allocation? Grids with more blocks will have more weights in the validation.

Response: Thanks for the comment. In our study, the patch-based samples focused more on assessing the mapping performance of our GLC-2015 map in heterogenous landscape, such as fragmented areas and transition zones. So, we used random sampling because this method is easy to perform and capable to increase the sample size from targeted areas (Pengra et al., 2020). In our study, we randomly selected 5 km × 5km patch-based samples over the globe and across different ecoregions. Subsequently, a manual adjustment was applied to slightly increased the sample size for areas with disagreement which exists in the previous GLC maps. In this way, the sample set is more capable to verify whether the GLC-2015 makes the improvement in regions where land cover is poorly mapped by pervious maps.

As the manual interpretation of large number of 5 km × 5 km blocks is time-consuming and labor-intensive, we generated 144 samples in the previous manuscript. Based on the suggestion, we have added another 57 5km× 5km samples to make the distribution more equal. In this way, the validation of our GLC-2015 map via patch-based samples will be more reliable.

We have updated the description of patch-based samples in our manuscript.

"Simple random sampling was used to derive 5 km × 5 km blocks over the world's terrestrial area and across different ecoregions because it is easy to perform and capable to augment the sample size from target areas (Pengra et al., 2020). Since inconsistency between current GLC maps tends to appear in those heterogeneous areas, such as fragmented regions and transition zones, we slightly increased the sample size for areas with the heterogeneous landscape to better evaluate our mapping results. In total, there were 201 blocks selected as the global patch-based samples, as displayed in Figure. 3a. Then, for each block in the patch-based samples, we used ArcGIS 10.5 software to derive polygons (patches) of various sizes which captured the real landscape on the high-resolution images. Meanwhile, each polygon was manually labeled with a LC class. Four examples of producing patch-based samples are shown in Figure. 3b-c.

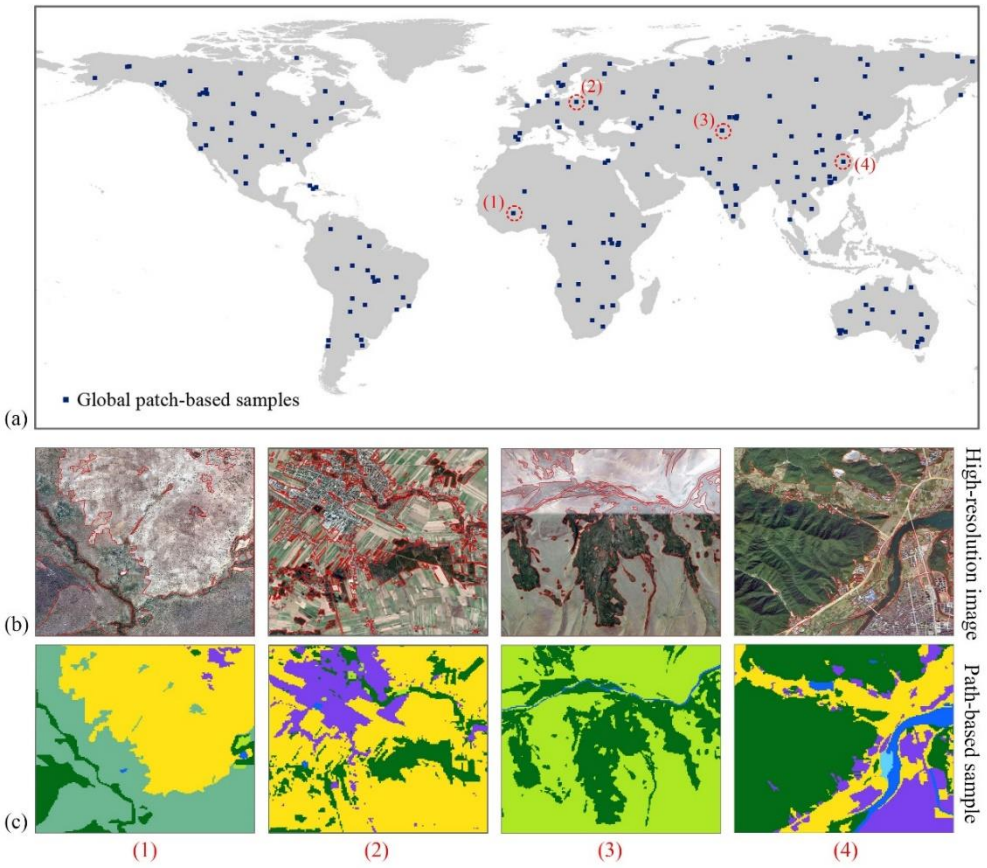

Figure 3. Spatial distribution and selected examples of the global patch-based samples. The locations of 5 km × 5 km patch-based samples are shown as panel (a), the locations of four selected samples are remarked by red dash circles. Panels (b) and (c) illustrate the production of global patch-based samples on manual interpretation. The red lines in high-resolution images circa 2015 are results after vectorization using ArcGIS 10.5 software. Four corresponding patch-based samples are shown as (c)." (Revised manuscript, Line 237-252)

In addition, all related validation results based on the global patch-based samples have been updated, including Table 4 and 6, Figure 9 and 10.

Table 4. Mapping accuracy via the global patch-based samples for the GLC-2015 map

	Cropland	Forest	Grassland	shrubland	Wetland	Water bodies	Tundra	Impervious surfaces	Bare land	Permanent snow and ice
PA	0.862	0.899	0.626	0.583	0.232	0.939	0.701	0.742	0.757	0.820
UA	0.917	0.814	0.634	0.687	0.647	0.916	0.872	0.722	0.617	0.751
OA	0.844									
Kappa	0.564									

Table 6. Mapping accuracy of the GLC products with the global patch-based samples

		Cropland	Forest	Grassland	Shrubland	Wetland	Water bodies	Tundra	Impervious surfaces	Bare land	Permanent snow and ice	OA (Kappa coefficient)
GLC-2015	PA	0.862	0.899	0.626	0.583	0.232	0.939	0.701	0.742	0.757	0.820	0.844
	UA	0.917	0.814	0.634	0.687	0.647	0.916	0.872	0.722	0.617	0.751	(0.564)
Globeland30	PA	0.896	0.698	0.765	0.539	0.455	0.824	0.752	0.643	0.492	0.831	0.735

	UA	0.891	0.906	0.444	0.527	0.157	0.893	0.500	0.703	0.829	0.705	(0.434)
FROM_GLC	PA	0.485	0.714	0.640	0.254	0.032	0.904	0.760	0.506	0.681	0.501	0.659
	UA	0.872	0.809	0.193	0.139	0.186	0.884	0.696	0.808	0.496	0.703	(0.353)
GLC_FCS30	PA	0.865	0.779	0.398	0.565	0.363	0.869	0.051	0.648	0.658	0.742	0.712
	UA	0.857	0.832	0.509	0.330	0.132	0.942	0.573	0.643	0.462	0.752	(0.414)

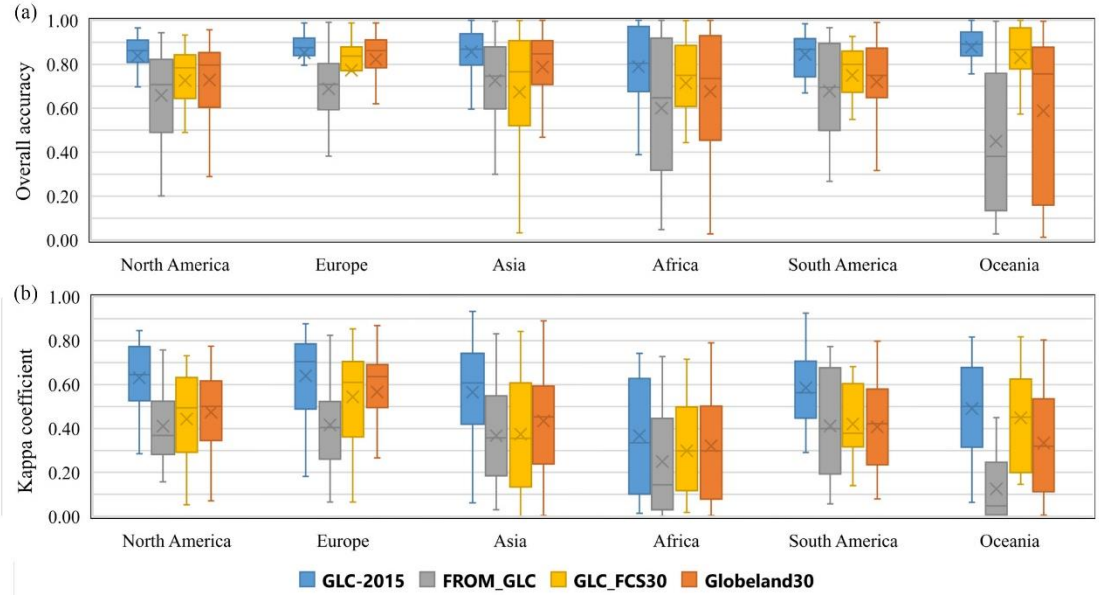

Figure 9. The box-plot of the accuracy for different continents. (a) overall accuracy, (b)kappa coefficient.

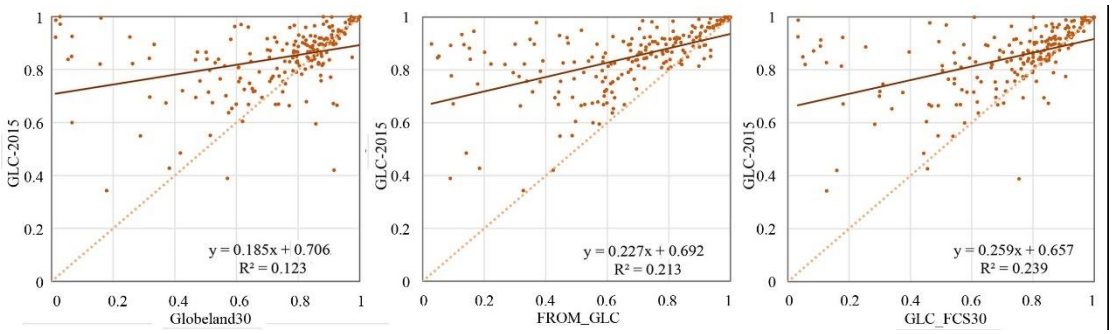

Figure 10. Scatter plots between the GLC-2015 map and other products obtained using the global patch-based samples.

References:

Pengra, B. W., Stehman, S. V., Horton, J. A., Dockter, D. J., Schroeder, T. A., Yang, Z., Cohen, W. B., Healey, S. P., and Loveland, T. R.: Quality control and assessment of interpreter consistency of annual land cover reference data in an operational national monitoring program, Remote Sens. Environ., 238, 111261, https://doi.org/10.1016/j.rse.2019.111261, 2020.

Comment #1-5. When I try to download your result, I found it was labeled by grid id. It would be better to label it with latitude and longitude (e.g., upper left corner), which is a straightforward and common way.

Response: Thanks for the suggestion. We have named the mapping result in each grid with latitude and longitude of its lower left corner and re-uploaded our results. Correspondingly, we have changed the description of our data as well as the access.

"The improved global land cover map in 2015 with 30 m resolution is available at https://doi.org/10.6084/m9.figshare.21371304.v1 (Li et al., 2022). The GLC-2015 product is organized by a total of 1507 4° × 4° geographical grids in GeoTIFF format across the world's terrestrial area. Each image of the GLC-2015 product is named as "GLC-2015_lon_lat" (lon and lat represent the longitude and latitude and of the grid's lower left corner, respectively)." (Revised manuscript, Line 771-775)

Comment #1-6. Echo to my comment above, I download a small file and load the smallest tile into my computer. I found a volcano (5.048 S, 151.330 E) in the Papua New Guinea was misclassified into water bodies. So, I further check the datasets you used. It turns out the error comes from the GLC_FCS30 and FROM-GLC (check the figure below). It indicates that your approach, despite the additional training samples, failed to correct such error. This may be a small problem when it comes to global mapping, and accidently found by me. But it's also a reminder for the authors to check their data and methods.

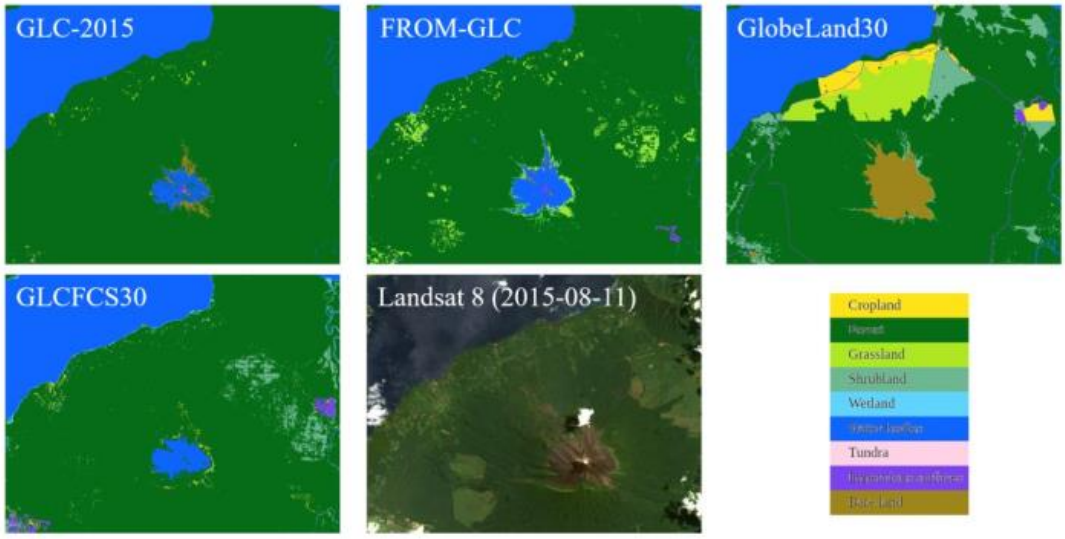

Response: Thanks for pointing out the error. Since the accuracy of our data reached 76.4% assessed with the global point-based samples and 84.4% with the global patch-based samples, it is inevitable that inaccurate classification exists, especially for small land cover. Although the GLC-2015 map was not capable of avoiding all the wrong mapping results, it proved to be superior to the existing products from the aspects of mapping accuracy for the easily misclassified classes and areas with great inconsistency. As advocated by previous work, the accuracy of the integrated map is expected to be improved with more high-quality data adopted (Fritz et al., 2011; Huang et al., 2022). To our knowledge, there are several LC products with 30m resolution at the national scale, such as the National Land Cover Database (NLCD) (Yang et al., 2018) and China's land-use/cover datasets (CLUDs) (Liu et al., 2014). These national LC maps are more likely to offer higher accuracy because they were produced by experts who have good knowledge of land cover classes nationally. Future work with these reliable products employed will help to avoid inaccurate classification of the fused product.

We have added the discussion about the uncertainties caused by the source data and the further work to improve the quality of our map. The detailed revision can be seen below.

"Although the GLC-2015 map can evidently improve mapping accuracy in inconsistent areas, there are still some problems. First, we used three multiple-class GLC maps and four single-class GLC maps as the source data for integration. Since those products provide information of land cover at the global scale, classification errors inevitably exist in some specific regions. The multisource product fusion method based on DEST depends highly on the quality of those candidate maps such that the inconsistency between those source maps might lead to incorrect classification." (Revised manuscript, Line 745-750)

"As advocated by researchers that the accuracy of the integrated map is expected to be improved with more high-quality data adopted in the mapping task (Fritz et al., 2011; Huang et al., 2022). Several land cover products which focus on a national scale are more likely to offer higher accuracy because they are produced by experts who have good knowledge of land cover classes nationally. Thus, more reliable national land cover products, such as the National Land Cover Database for the year 2016 (NLCD2016) (Yang et al., 2018) and China's land-use/cover datasets (CLUDs) in 2015 (Liu et al., 2014), can further be integrated by our proposed method to develop a more accurate GLC map." (Revised manuscript, Line 763-769)

References:

Fritz, S., You, L., Bun, A., See, L., McCallum, I., Schill, C., Perger, C., Liu, J., Hansen, M., and Obersteiner, M.: Cropland for sub-Saharan Africa: A synergistic approach using five land cover data sets, Geophy. Res. Lett., 38, L04404, https://doi.org/10.1029/2010GL046213, 2011.

Huang, A., Shen, R., Li, Y., Han, H., Di, W., and Hagan, D. F.: A methodology to generate integrated land cover data for land surface model by improving Dempster-Shafer theory, Remote Sen., 14, 972, https://10.3390/rs14040972, 2022.

Liu, J., Kuang, W., Zhang, Z., Xu, X., Qin, Y., Ning, J., Zhou, W., Zhang, S., Li, R., Yan, C., Wu, S., Shi, X., Jiang, N., Yu, D., Pan, X., and Chi, W.: Spatiotemporal characteristics, patterns and causes of land use changes in China since the late 1980s, Dili Xuebao/Acta Geogr. Sin., 69, 3-14, https://doi.org/10.11821/dlxb201401001, 2014.

Yang, L., Jin, S., Danielson, P., Homer, C., Gass, L., Bender, S. M., Case, A., Costello, C., Dewitz, J., Fry, J., Funk, M., Granneman, B., Liknes, G. C., Rigge, M., and Xian, G.: A new generation of the United States National Land Cover Database: Requirements, research priorities, design, and implementation strategies, ISPRS J. Photogramm. Remote Sens., 146, 108-123, https://doi.org/10.1016/j.isprsjprs.2018.09.006, 2018.

Comment #1-7. GLC_FCS30 adopted a detailed classification system (level-2) only in some places (seems to inherit from the ESA CCI_LC). Therefore, I think this may lead to geographical accuracy biases even after you remap the level-2 LCs to yours. How did you deal with it, could you clarify?

Response: Thanks for the comment. We agree that there may be geographical accuracy biases from GLC_FCS30. We are sorry that we just remapped level-2 classes to match the land cover classes in our classification system without dealing with the biases because we have no effective strategy to address this problem. In our study, we collected a total number of 20,000 point-based samples over the globe and

used 80% of the samples to evaluate the accuracy of each GLC product. If the GLC_FCS30 has lower quality than other products in some regions, the LC classes from it will not be assigned to the output map. In this way, the uncertainties brought by the geographical accuracy biases of the GLC_FCS30 can be decreased. In the future, efforts will be made to solve this problem.

We have discussed this issue in the manuscript as follows:

"Third, there might be geographical accuracy biases from the GLC_FCS30 since it adopted a detailed level-2 classification system only for some areas. In this study, we used sufficient point-based samples to assess the accuracy of different GLC products. Based on the evaluation, LC classes could be selected from other more reliable candidate maps if the GLC_FCS30 provided low accuracy. In this way, the uncertainty brought by GLC_FCS30 could be reduced to some extent." (Revised manuscript, Line 758-762)

Comment #1-8. The accuracy assessment of your results shows the same pattern with the existing ones, where some LCs (e.g., shrub and wetland) always possess lower accuracies. Geographically, both your results and existing ones exhibit poor performance in areas with more disagreements (Table 7). I don't see much contribution and improvements in this dataset.

Response: Thanks for the comment. Our map showed relatively low accuracy for some land cover classes, such as shrubland, grassland, and wetland. However, it still provided more accurate information than the current 30m-resolution GLC maps with the PA and OA ranking first or second for those LC classes (see Table 5 and Table 6, the accuracy of the GLC-2015 ranks first is underlined with purple and the second with green).

The grassland is easy to be misclassified with cropland in some specific regions due to the high phenological similarity between them. Shrubland is mainly confused with forest due to similar spectral information and ambiguous definition. As for wetland, it is often mixed with vegetation and water bodies due to their complex spectral characteristics. It is a great challenge to accurately map those LC classes when generating a multiple-class GLC product (Liu et al., 2021; Zhang et al.,2021). With more reliable products for these three LC classes available, we can improve the mapping performance for them using our multi-source product fusion method.

Table 5. Mapping accuracy of the GLC products with the global point-based samples.

		Cropland	Forest	Grassland	Shrubland	Wetland	Water bodies	Tundra	Impervious surfaces	Bare land	Permanent snow and ice	OA (Kappa coefficient)
GLC-2015	PA	0.741	0.917	0.658	0.358	0.399	0.856	0.667	0.857	0.857	0.881	0.760
	UA	0.854	0.783	0.440	0.762	0.673	0.839	0.832	0.780	0.772	0.932	(0.715)
Globeland30	PA	0.749	0.712	0.651	0.208	0.508	0.681	0.770	0.681	0.591	0.806	0.635
	UA	0.770	0.805	0.220	0.386	0.521	0.870	0.575	0.790	0.864	0.907	(0.576)
FROM_GLC	PA	0.385	0.694	0.705	0.389	0.347	0.592	0.705	0.751	0.723	0.875	0.613
	UA	0.647	0.862	0.269	0.418	0.282	0.753	0.687	0.646	0.774	0.763	(0.554)
GLC_FCS30	PA	0.744	0.764	0.389	0.354	0.439	0.600	0.227	0.777	0.783	0.712	0.635
	UA	0.596	0.798	0.314	0.385	0.471	0.804	0.688	0.758	0.637	0.948	(0.568)

Table 6. Mapping accuracy of the GLC products with the global patch-based samples

		Cropland	Forest	Grassland	Shrubland	Wetland	Water bodies	Tundra	Impervious surfaces	Bare land	Permanent snow and ice	OA (Kappa coefficient)
GLC-2015	PA	0.862	0.899	0.626	0.583	0.232	0.939	0.701	0.742	0.757	0.820	0.844
	UA	0.917	0.814	0.634	0.687	0.647	0.916	0.872	0.722	0.617	0.751	(0.564)
Globeland30	PA	0.896	0.698	0.765	0.539	0.455	0.824	0.752	0.643	0.492	0.831	0.735
	UA	0.891	0.906	0.444	0.527	0.157	0.893	0.500	0.703	0.829	0.705	(0.434)
FROM_GLC	PA	0.485	0.714	0.640	0.254	0.032	0.904	0.760	0.506	0.681	0.501	0.659
	UA	0.872	0.809	0.193	0.139	0.186	0.884	0.696	0.808	0.496	0.703	(0.353)
GLC_FCS30	PA	0.865	0.779	0.398	0.565	0.363	0.869	0.051	0.648	0.658	0.742	0.712
	UA	0.857	0.832	0.509	0.330	0.132	0.942	0.573	0.643	0.462	0.752	(0.414)

When it comes to the mapping performance of our GLC-2015 map in areas with different-level disagreements, our map had worse performance in areas with more disagreements, as shown in Table 7. However, our map outperformed the other three in both areas of low inconsistency, moderate inconsistency, and high inconsistency. Especially, the accuracy gain of our map against other products was **21.0%-25.2%** for areas of high inconsistency, which was larger compared to 17.6%-23.2% for areas of moderate inconsistency and 0.2%-1% for areas of low inconsistency. That is to say, the superiority of our map over others is more evident in areas with more disagreements. So, we can conclude that the GLC-2015 map obtains great improvement and provides a more accurate characterization of land cover in poorly-mapped areas.

Table 7. Accuracy assessments of the GLC products in three areas.

	GLC-2015		Globeland30		FROM_GLC		GLC_FCS30	
	OA	Kappa	OA	Kappa	OA	Kappa	OA	Kappa
Areas of low inconsistency	0.939	0.922	0.931	0.912	0.929	0.909	0.937	0.919
Areas of moderate inconsistency	0.717	0.671	0.534	0.467	0.485	0.416	0.541	0.464
Areas of high inconsistency	**0.509**	0.430	**0.285**	0.196	**0.299**	0.212	**0.257**	0.144

In addition, based on the suggestion of another reviewer, we have added the comparison of the accuracy of the GLC-2015 map and mapping results from other data fusion methods and RF classifier. The details can be found in the **Comment #2-1** and **Comment #2-2**.

Reviewer #2:

This paper developed an improved global land cover map at 30m resolution in 2015 by fusing multi-source products of land covers and other thematic mappers. Two sets of global samples with points and patches have been developed and used to evaluate the performance of derived GLC-2015. This work is high-intensive in terms of the labor involved, and the evaluation is sound with clear logic. Before recommending it for publication, I raised several concerns below, which might be helpful to improve this paper.

Response: We thank the reviewer for the comments. These comments are very helpful for revising and improving our paper. The manuscript has been improved according to your and another reviewer's comments. The point-by-point responses are listed below in **blue**. The changes in our manuscript are marked with red.

Comment #2-1. Although the authors adopted the DSET approach to generate the GLC-2015 product and compared it with similar products such as FROM-GLC and GLC_FCS30, the improvements gained from the DSET approach should be highlighted in those common approaches such as major voting and other common approaches. Otherwise, the highlights of the DSET in the manuscript should be reconsidered.

Response: Thanks for the comment. Based on the suggestion, we have highlighted the advantage of the DSET as follows: (1) The DSET method can discount evidence form inaccurate information with a probability mass that reflects the degree of belief rather than a binary decision (Razi et al., 2019); (2) The DSET can integrate evidence from a variety of sources without the requirement of prior knowledge (Chen and Venkataramanan, 2005); (3) The DSET method can provide a total degree of belief to reflect the reliability of the final fused results.

Correspondingly, we have added this part in Introduction Section:

"Several attempts have been made to produce an accurate and consistent LC map using various methods, such as majority voting (MV), fuzzy agreement and Bayesian theory. Iwao et al. (2011) created a GLC map based on a simple majority voting method. Jung et al. (2006) generated a 1km GLC map by combination of MODIS, GLC2000 and GLCC data based on fuzzy agreement scoring. Subsequently, Fritz et al. (2011) extended the synergy method of Jung et al. (2006) by ranking LC maps and mapped the cropland extent in Sub-Saharan Africa. See et al. (2015) generated two GLC products by integrating medium resolution LC products with geographically weighted regression (GWR). Gengler and Bogaert (2018) proposed a Bayesian data fusion method and applied it to the LC mapping for a specific region in Belgium. All these researches have demonstrated that fusion method can create an integrated LC product where the mapping accuracy is greatly improved by combing the best of candidate maps. However, the MV method is sensitive to the quality of the candidate maps and has significant uncertainties when the input products exhibit great disagreement(Chen and Venkataramanan, 2005). The fuzzy agreement is highly subjective since it depends on expert assessment, while the Bayesian theory requires a prior knowledge or conditional probabilities and fails to handle the states of ignorance(Liu and Xu, 2021).

The Dempster-Shafer theory of evidence (DSET) is an evidence-based approach to reason with uncertainties. Unlike the majority voting, the DSET method can discount evidence form inaccurate information with a probability mass that reflects the degree of belief rather than a binary decision (Razi

et al., 2019). In contrast to the Bayesian theory, the DSET can integrate evidence from a variety of sources without the requirement of prior knowledge (Chen and Venkataramanan, 2005). Moreover, the reliability of the final fused results is measured by the DSET method with a total degree of belief. Although previous literature focused on the application of the DSET method in multisource data aggregation, very little research has been conducted at a global scale due to the lack of accurate and sufficient samples and the demand for adequate computing resources." (Revised manuscript, Line 93-115)

Furthermore, we have compared the DSET and other data fusion methods in our revised manuscript. Comparison shows the superiority of the DSET over other methods. First, we added how we conducted the comparison in Section 3 as follows:

"**3.5 Assessment on mapping performance of DSET and other methods**

In addition to inter-comparison between the GLC-2015 map and three existing GLC products, we compared the DSET method with two existing commonly used fusion methods, including the majority voting (MV) and spatial correspondence (SC) based on two global validation sets including 20% of the global point-based samples and the whole global patch-based samples. MV is a fusion approach that combines input maps and adopts the LC class favored by the majority of the candidate maps. In the MV method, we compared the GlobeLand30, FROM_GLC, and GLC_FCS30 at each pixel and chose the class that two or three LC products agreed for. For pixels where three LC products were different, the LC class of the product with the highest accuracy was adopted. SC method produces an integrated land cover map by selecting the LC class of the input map that has the highest spatial correspondence with the reference data. In this study, 80% of the global point-based samples were used as the reference data to obtain the SC map of each global LC product. If the class of a product agreed with that of the point-based sample, a value equal to 1 was assigned to that sample. On the contrary, a value equal to 0 was assigned to the sample if the class of the product differed from that of the sample. In each 4° × 4° grid, we used the Kriging method to obtain spatial correspondence maps which have the correspondence value ranging from 0 to 1 for three products. Then, the class of the product with the highest spatial correspondence was chosen for each pixel." (Revised manuscript, Line 402-418)

Then we have added the assessment on the DSET and other two methods in Section 4 as well as supplementary material.

"4.5.1 Inter-comparison with other data fusion methods

The accuracy assessments on GLC-2015 obtained by DSET and global mapping results from two other data fusion methods were conducted based on two global validation sample sets. The error matrices with the global point-based samples are shown in Table S3 and S4. The OA of the global land cover classification obtained by the MV and SC was 69.9% and 71.9%, respectively. As shown in Table 3, the OA of the GLC-2015 map obtained by the DSET method was 76.0%, which had an improvement of 6.1% and 4.1% compared to mapping results from the MV and SC. In addition, the GLC-2015 map obtained higher PA and UA for most LC classes." (Revised manuscript, Line 670-677)

"**Table S3. The error metric for the land cover classification obtained by MV method based on the global point-based samples.**

	Cropland	Forest	Grassland	Shrubland	Wetland	Water bodies	Tundra	Impervious	Bare land	Permanent	Total	PA

								surfaces		snow and ice		
Cropland	3491	200	572	169	29	23	6	80	80	0	4650	0.751
Forest	541	7642	357	568	279	24	37	78	119	2	9847	0.792
Grassland	173	206	1634	176	57	10	16	45	134	1	2452	0.666
Shrubland	426	469	937	1184	82	10	38	45	431	0	3622	0.327
Wetland	113	296	88	81	809	70	32	10	143	3	1645	0.492
Water bodies	140	123	38	56	131	1501	65	17	176	4	2251	0.667
Tundra	0	134	173	115	10	17	1300	1	331	3	2084	0.624
Impervious surfaces	123	12	24	19	5	3	3	1264	42	0	1495	0.854
Bare land	163	26	486	210	61	48	67	88	4476	9	5634	0.794
Permanent snow and ice	3	8	27	10	9	37	17	2	121	902	1136	0.794
Total	5173	9116	4336	2588	1472	1743	1581	1630	6053	924	34616	
UA	0.675	0.838	0.377	0457	0.550	0.861	0.822	0.775	0.739	0.976		
OA						0.699						
Kappa						0.646						

Table S4. The error metric for the land cover classification obtained by SC method based on the global point-based samples.

	Cropland	Forest	Grassland	Shrubland	Wetland	Water bodies	Tundra	Impervious surfaces	Bare land	Permanent snow and ice	Total	PA
Cropland	3144	133	869	243	69	24	10	67	91	2	4652	0.676
Forest	285	7524	628	737	155	19	149	80	47	23	9647	0.780
Grassland	99	84	1864	150	43	14	70	40	78	12	2454	0.760
Shrubland	216	181	1043	1603	66	30	86	74	318	11	3628	0.442
Wetland	41	252	383	117	703	38	58	16	32	5	1645	0.427
Water bodies	64	95	75	36	249	1556	47	33	83	8	2246	0.693
Tundra	9	46	102	55	53	13	1711	2	80	14	2085	0.821
Impervious surfaces	66	6	44	13	9	7	5	1261	80	5	1496	0.843
Bare land	51	30	447	131	132	104	91	66	4544	42	5638	0.806
Permanent snow and ice	1	4	17	1	11	18	26	0	46	1008	1132	0.890
Total	3976	8355	5472	3086	1490	1823	2253	1639	5399	1130	34623	
UA	0.791	0.901	0.341	0.519	0.472	0.854	0.759	0.769	0.842	0.892		
OA						0.719						
Kappa						0.674						

” (Supplementary material with change)

“When evaluating GLC maps obtained by different data fusion approaches using the global patch-based samples, the DSET method obtained the highest OA of 84.4% and kappa coefficient of 0.564, compared with 80.1% and 0.497 for MV, and 71.8% and 0.391 for SC (Table S5). Here, the DSET method achieved an accuracy improvement of 4.3% and 12.6%. Compared to the two other methods, the DSET improved the accuracy for nearly all the LC classes, especially for grassland, shrubland, and wetland. We also compared the overall accuracy relationship between the DSET and other methods. From the scatter plots (Figure 15), we found that the majority of points were above the 1:1 line, implying DSET had better mapping performance than others in most regions across the globe.

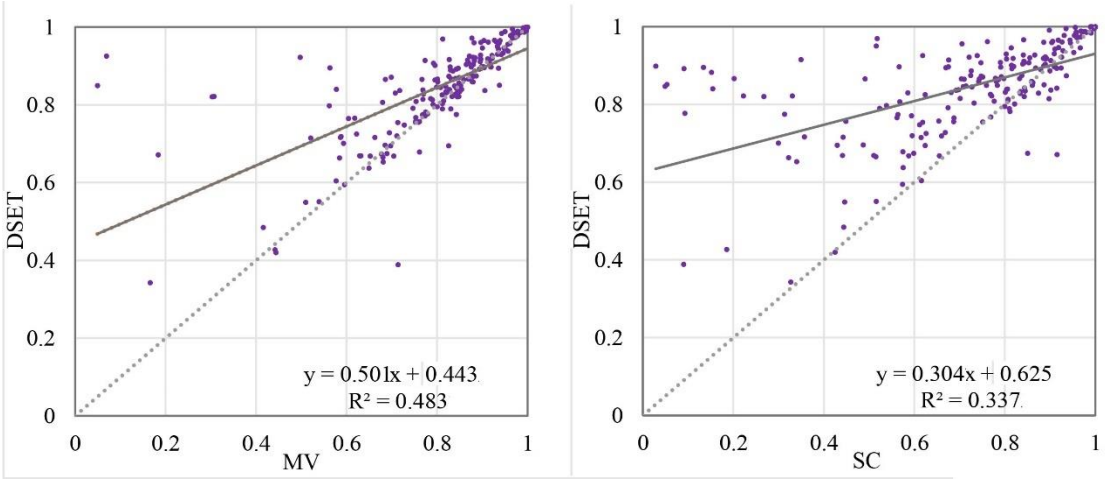

Figure 15. Scatter plots between the DSET and other data fusion methods based on the global patch-based samples." (Revised manuscript, Line 678-688)

"**Table S5. Mapping accuracy of different data fusion methods with the global patch-based samples**

		Cropland	Forest	Grassland	Shrubland	Wetland	Water bodies	Tundra	Impervious surfaces	Bare land	Permanent snow and ice	OA (Kappa coefficient)
DSET	PA	0.862	0.899	0.626	0.583	0.232	0.939	0.701	0.742	0.757	0.820	0.844
	UA	0.917	0.814	0.634	0.687	0.647	0.916	0.872	0.722	0.617	0.751	(0.564)
MV	PA	0.891	0.872	0.580	0.452	0.172	0.930	0.831	0.709	0.620	0.779	0.801
	UA	0.890	0.882	0.569	0.448	0.166	0.944	0.827	0.717	0.612	0.779	(0.497)
SC	PA	0.877	0.856	0.276	0.177	0.178	0.870	0.803	0.690	0.472	0.675	0.718
	UA	0.885	0.869	0.268	0.171	0.180	0.883	0.769	0.707	0.473	0.675	(0.391)

" (Supplementary material with change)

"Land cover mapping results from the DSET and other methods were also visually illustrated in six tiles with size of the 0.25° covering different continents, as displayed in Figure S4. Despite that mapping results from the DSET and MV depicted similar spatial distribution of LC classes in all tiles except the tile in North America, the DSET more accurately delineated the impervious surfaces of small size which scattered in cropland-dominated (Figure S4a) or arid areas (Figure S4c). Notably, the mapping results from the SC method presented significant differences from that obtained by the DSET and MV. For example, the SC method failed to capture scattered rural residential areas (Figure S4b) and misclassified grassland as cropland (Figure S4d). Overall, the DSET method possessed better recognition performance in various LC classes than the other two methods." (Revised manuscript, Line 689-697)

"

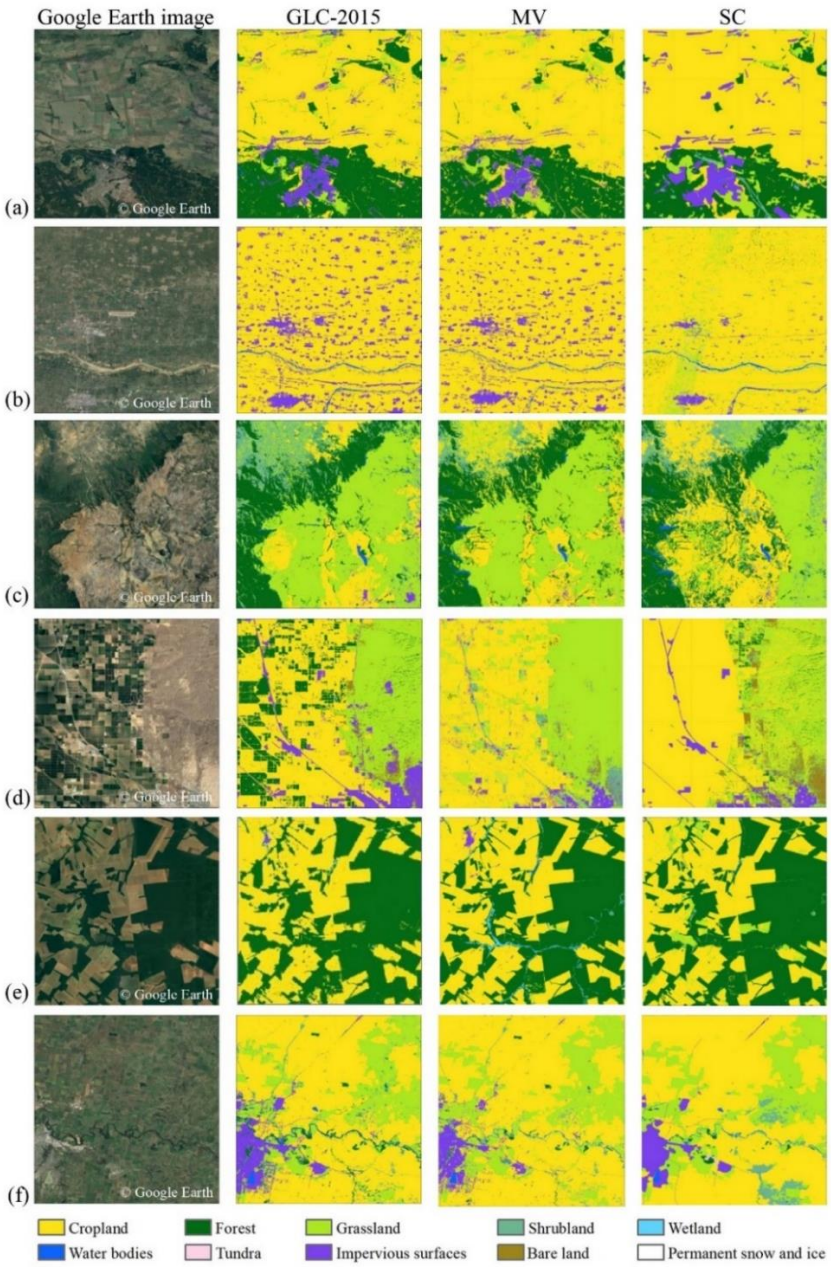

Figure S4. Visual comparison between mapping results from DSET and other data fusion methods for different continents. (a) to (f) are examples for Europe, Asia, Africa, North America, South America, and Oceania, respectively." (Supplementary material with change)

"In summary, from the respective of both two global validation sets, the LC map from DSET (GLC-2015) obtained higher OA and performed better in identifying different classes related to those from two others, which demonstrated that the DSET method we adopted is robust to generate a new LC map from the existing products. Especially, the OA of the MV and SC was also higher than the Globeland30, FROM_GLC, and GLC_FCS30, confirming that higher accuracy could be achieved by integrating various LC maps." (Revised manuscript, Line 698-703)

Third, we emphasized the superiority of the DSET over other methods in the Section 6.

"In addition, the mapping results obtained by the DSET surpassed other data fusion methods with OA

improvement of 4.1%-6.1% via the global point-based samples and 4.3%-12.6% via the global patch-based samples. Therefore, it can be concluded that the GLC-2015 map is a robust and reliable map that can significantly improve mapping accuracy compared to previous GLC products and mapping results from other common data fusion methods." (Revised manuscript, Line 796-801)

References:

Chen, T. M. and Venkataramanan, V.: Dempster-Shafer theory for intrusion detection in ad hoc networks, IEEE Internet computing, 9, 35-41, https://doi.org/10.1109/MIC.2005.123, 2005.

Liu, K. and Xu, E.: Fusion and correction of multi-source land cover products based on spatial detection and uncertainty reasoning methods in Central Asia, Remote Sen., 13, 244, https://doi.org/10.3390/rs13020244, 2021.

Gengler, S. and Bogaert, P.: Combining land cover products using a minimum divergence and a Bayesian data fusion approach, Int. J. Geogr. Inf. Sci. , 32, 806-826, https://doi.org/10.1080/13658816.2017.1413577, 2018.

Iwao, K., Nasahara, K. N., Kinoshita, T., Yamagata, Y., Patton, D., and Tsuchida, S.: Creation of new global land cover map with map integration, J. Geogr. Inf. Syst., 3, 160-165, https://doi.org/10.4236/jgis.2011.32013, 2011.

Jung, M., Henkel, K., Herold, M., and Churkina, G.: Exploiting synergies of global land cover products for carbon cycle modeling, Remote Sens. Environ., 101, 534-553, https://doi.org/10.1016/j.rse.2006.01.020, 2006.

Razi, S., Karami Mollaei, M. R., and Ghasemi, J.: A novel method for classification of BCI multi-class motor imagery task based on Dempster–Shafer theory, Inf. Sci., 484, 14-26, https://doi.org/10.1016/j.ins.2019.01.053, 2019.

See, L., Schepaschenko, D., Lesiv, M., McCallum, I., Fritz, S., Comber, A., Perger, C., Schill, C., Zhao, Y., Maus, V., Siraj, M. A., Albrecht, F., Cipriani, A., Vakolyuk, M. y., Garcia, A., Rabia, A. H., Singha, K., Marcarini, A. A., Kattenborn, T., Hazarika, R., Schepaschenko, M., van der Velde, M., Kraxner, F., and Obersteiner, M.: Building a hybrid land cover map with crowdsourcing and geographically weighted regression, ISPRS J. Photogramm. Remote Sens., 103, 48-56, https://doi.org/10.1016/j.isprsjprs.2014.06.016, 2015.

Comment #2-2. How about the mapping performance if using these samples (80%) do the classification directly? Because these samples have been manually visualized and are qualified for the classification task. Please add some test results or discuss this issue in the manuscript.

Response: Thanks for the comment. Based on the suggestion, we have added the test results of the classification using the Random Forest classifier trained on the 80% of the global point-based samples in our revised manuscript. The detailed revision can be seen below.

"In addition to the comparison between DSET and two other fusion methods, we compared the mapping performance of DSET with Random Forest (RF) which is considered one of the most popular algorithms for land cover mapping. In the land cover classification using the FR classifier, all available Level-2 Tier 1surface reflectance (SR) data of Landsat 8 OLI (Operational Land Imager) sensors from the year 2015 and two adjacent years on GEE was employed. All Landsat images have been atmospherically corrected.

The following six bands were used as input features: blue, green, red, NIR, SWIR1, and SWIR2. To improve the mapping performance, several important spectral indices, including DNVI, NDWI, and NDBI were also used as auxiliary data to the RF classifier. The RF classifier was trained on 80% of the global point-based samples since those samples were of high quality after manual visual interpretation of high-resolution images. As the global land cover mapping based on the RF classifier is a tough task, we randomly selected a total of 300 grids with the size of 4° (Figure S1) and used corresponding local classifiers to these grids. Then, the mapping results were validated by the remaining 20% of the global-point samples." (Revised manuscript, Line 419-431)

"

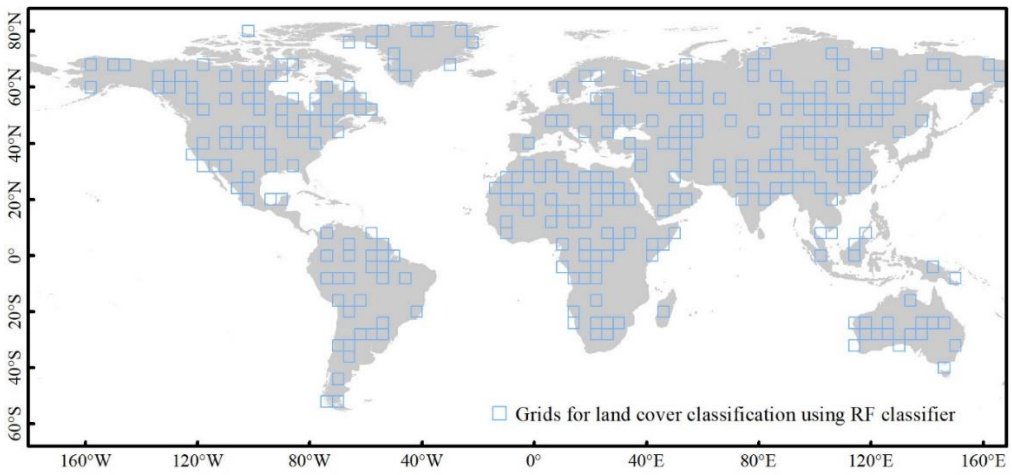

Figure S1. The spatial distribution of the selected 4° × 4° grids where the comparison between DSET and RF classifier was implemented." (Supplementary material with change)

"4.5.2 Inter-comparison with the Random Forest

Based on the validation data from 20% of the global point-based samples, we evaluated the quality of the GLC-2015 map obtained by the DSET method and mapping results classified by the RF classifier for a total of 300 grids. The DSET method obtained an average OA of 77.7% across six continents, while the RF achieved a lower accuracy of 69.8%. From the scatter plots which compared the OA and kappa coefficient between the DSET and RF grid by grid, we can see that the DSET possessed higher accuracy in most grids (Figure S5). Especially, the points were clustered in the upper right corner of the plot (Figure S5a), which indicated that the RF classifier trained with the global point-based samples performed well in those selected grids though it was inferior to the DSET method. Figure S6 shows the OA of the DSET and RF across six continents. We found that the DSET method outperformed RF classifier for each continent. Additionally, the DSET was similar to the RF in terms of the ranking of accuracy over the continents. Especially, the mapping results of both two methods presented the lowest accuracy in Oceania. It may be because the selected grids were located in regions with heterogeneous landscape. As for the box plot for the RF classifier, the low hinge exceeded 60.00% in all continents except Oceania, demonstrating the reliability of the RF classifier trained by the global point-based samples. Nevertheless, the performance of the RF classifier was worse than the DSET method. This highlights the feasibility of the DSET method in integrating the existing maps for a better one." (Revised manuscript, Line 704-720)

"

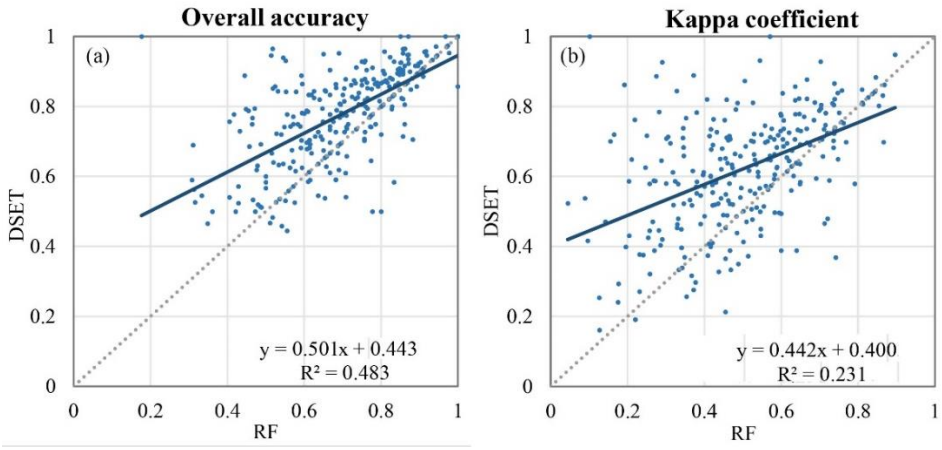

Figure S5. Scatter plots between the DSET and RF based on the global point-based samples.

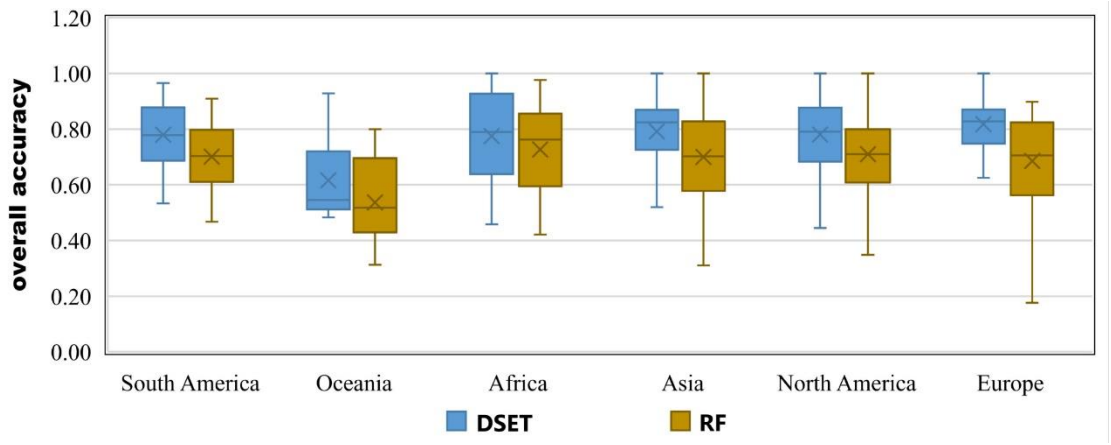

Figure S6. The box plot of the overall accuracy comparison between the DSET and RF for different continents." (Supplementary material with change)

Comment #2-3. The proposed work can also be applied in regions with adequate and high-quality data, such as NLCD in the US and China. This can be improved or discussed in the revised manuscript.

Response: Thanks for the suggestion. We have added the section 4.6 "Advancement and Limitations" in our manuscript and discussed future work based on more high-quality data.

"Although the GLC-2015 map can evidently improve mapping accuracy in inconsistent areas, there are still some uncertainties. First, we used three multiple-class GLC maps and four single-class GLC maps as the source data for integration. Since those products are created for providing information of land cover at the global scale, classification errors will inevitably exist in some specific regions. The multisource product fusion method based on DEST depends highly on the quality of those candidate maps such that the inconsistency between those source maps might lead to incorrect classification." (Revised manuscript, Line 745-750)

"As advocated by researchers that the accuracy of the integrated map is expected to be improved with more high-quality data adopted in the mapping task (Fritz et al., 2011; Huang et al., 2022). Several land cover products which focus on a national scale are more likely to offer higher accuracy because they are produced by experts who have good knowledge of land cover classes nationally. Thus, more reliable

national land cover products, such as the National Land Cover Database for the year 2016 (NLCD2016) (Yang et al., 2018) and China's land-use/cover datasets (CLUDs) in 2015 (Liu et al., 2014), can further be integrated by our proposed method to develop a more accurate GLC map." (Revised manuscript, Line 763-769)

References:

Fritz, S., You, L., Bun, A., See, L., McCallum, I., Schill, C., Perger, C., Liu, J., Hansen, M., and Obersteiner, M.: Cropland for sub-Saharan Africa: A synergistic approach using five land cover data sets, Geophys. Res. Lett., 38, L04404, https://doi.org/10.1029/2010GL046213, 2011.

Huang, A., Shen, R., Li, Y., Han, H., Di, W., and Hagan, D. F.: A methodology to generate integrated land cover data for land surface model by improving Dempster-Shafer theory, Remote Sen., 14, 972, https://doi.org/10.3390/rs14040972, 2022.

Liu, J., Kuang, W., Zhang, Z., Xu, X., Qin, Y., Ning, J., Zhou, W., Zhang, S., Li, R., Yan, C., Wu, S., Shi, X., Jiang, N., Yu, D., Pan, X., and Chi, W.: Spatiotemporal characteristics, patterns and causes of land use changes in China since the late 1980s, Dili Xuebao/Acta Geogr. Sin., 69, 3-14, https://doi.org/10.11821/dlxb201401001, 2014.

Yang, L., Jin, S., Danielson, P., Homer, C., Gass, L., Bender, S. M., Case, A., Costello, C., Dewitz, J., Fry, J., Funk, M., Granneman, B., Liknes, G. C., Rigge, M., and Xian, G.: A new generation of the United States National Land Cover Database: Requirements, research priorities, design, and implementation strategies, ISPRS J. Photogramm. Remote Sens., 146, 108-123, https://doi.org/10.1016/j.isprsjprs.2018.09.006, 2018.

Minor Comments:

Comment #2-4. Page 108: BPA function. This term should be fully spelled when it first appears in the main text.

Response: Thanks for the comment. The full name of the term has been added at the place it first appears in the revised manuscript.

"To fulfill the purpose, we first performed reliability evaluation, where the accuracy of each GLC product for each LC class in each 4° × 4° geographical grid is regarded as the evidential probability to create the basic probability assignment (BPA) function." (Revised manuscript, Line121-123)

Comment #2-5. Page 172: The selection of 4°×4° should be discussed.

Response: Thanks for the comment. For large-scale or global land cover mapping, previous researchers divided the study area into a lot of sub-regions (Gong et al., 2020; Huang et al.,2021; Jin et al., 2022; Liu et al., 2020; Zhang et al., 2020,2021; Zhao et al.,2021). When applying the DSET method to generate a global hybrid map, it is more useful to use the local adaptive fusion model for each sub-regions rather than a single model for the whole globe. We divided the global land into 4°×4° sub-regions with the following two considerations:

(1) Sufficiency of samples for land cover classes. If we generate the samples in a small spatial grid such as a Landsat scene, the size of samples might be insufficient and it was also difficult to obtain samples

for the rare land cover classes.

(2) Computation capacity and memory of the GEE platform. The GEE platform provides unprecedented opportunities for global land cover classification tasks due to the access to numerous analysis-ready earth observations datasets and high-performance, intrinsically parallel computation (Gorelick et al., 2017). However, GEE has computation capacity limitations. It is impossible to implement mapping work at a sub-region as large as we want because of the issue of running out of memory.

In our study, to balance the mapping efficiency on the GEE platform and the sufficiency for land cover classes in sub-regions, we split the globe into 1507 4°×4° geographical grids and then conducted land cover mapping at the regional scale.

Correspondingly, we have added the explanation for dividing the world's terrestrial area into 4°×4° grids.

"For large-scale or global land cover mapping, previous researchers divided the study area into a lot of sub-regions and conducted classification in each sub-region on GEE (Gong et al., 2020; Liu et al., 2020; Huang et al., 2021; Jin et al., 2022; Zhang et al., 2021; Zhao et al., 2021). The shape and size of sub-region vary in previous work, such as hexagons with a side length of 2°, geographical grids with a size of 1°×1°, 3.5°×3.5°, 5°×5°, or 10°×10°. When deciding on the size of sub-regions, two important factors should be considered. The size of samples in each sub-region should be sufficient so that the rare land cover classes will not be missed. On the other hand, it is impossible to implement mapping work at a sub-region as large as we want due to memory constraints. To balance the mapping efficiency on the GEE platform and the sufficiency for land cover classes, we split the world's terrestrial area into 1507 4°×4° geographical grids." (Revised manuscript, Line 262-271)

References:

Gong, P., Li, X., Wang, J., Bai, Y., Chen, B., Hu, T., Liu, X., Xu, B., Yang, J., Zhang, W., and Zhou, Y.: Annual maps of global artificial impervious area (GAIA) between 1985 and 2018, Remote Sens. Environ., 236, 111510, https://doi.org/10.1016/j.rse.2019.111510, 2020.

Gorelick, N., Hancher, M., Dixon, M., Ilyushchenko, S., Thau, D., and Moore, R.: Google Earth Engine: Planetary-scale geospatial analysis for everyone, Remote Sens, Environ., 202, 18–27, https://doi.org/10.1016/j.rse.2017.06.031, 2017.

Huang, X., Li, J., Yang, J., Zhang, Z., Li, D., and Liu, X.: 30m global impervious surface area dynamics and urban expansion pattern observed by Landsat satellites: From 1972 to 2019., Sci. China Earth Sci, 64, 1922–1933, https://doi.org/10.1007/s11430-020-9797-9, 2021.

Jin, Q.; Xu, E.; and Zhang, X.: A fusion method for multisource land cover products based on superpixels and statistical extraction for enhancing resolution and improving accuracy, Remote Sens, 14, 1676, https://doi.org/10.3390/rs14071676, 2022.

Liu, X., Huang, Y., Xu, X., Li, X., Li, X., Ciais, P., Lin, P., Gong, K., Ziegler, A. D., Chen, A., Gong, P., Chen, J., Hu, G., Chen, Y., Wang, S., Wu, Q., Huang, K., Estes, L., and Zeng, Z.: High-spatiotemporal-resolution mapping of global urban change from 1985 to 2015, Nature Sustainability, 3, 564-570, https://doi.org/10.1038/s41893-020-0521-x, 2020.

Zhang, X., Liu, L., Chen, X., Gao, Y., Xie, S., and Mi, J.: GLC_FCS30: global land-cover product with fine classification system at 30 m using time-series Landsat imagery, Earth Syst. Sci. Data, 13, 2753-2776, https://doi.org/10.5194/essd-13-2753-2021, 2021.

Zhao, J., Yu, L., Liu, H., Huang, H., Wang, J., and Gong, P.: Towards an open and synergistic framework for mappingglobal land cover, PeerJ, 9, e11877, https://doi.org/10.7717/peerj.11877, 2021.

Comment #2-6. Page 178-179: I wonder why the initial samples generated from the FROM_GLC were used in this study, not other land cover products. Explanations about this topic should be discussed in the manuscript.

Response: Thanks for the comment. Collecting global point-based samples is a key step in our study. We employed stratified random sampling which generates samples for land cover classes based on area proportion from reference land cover product. In this method, a classification map served as prior knowledge. This map was only used to derive proper size for each class. The reasons why we chose the FROM_GLC as the reference map other than Globeland30 and GLC_FCS30 are as follows:

(1) From the respective of time, the data time of Globeland30 product is 2010 which has a 5-year interval from our samples. If we used Globeland30, there would be some land cover change between 2010 and 2015 and the size of samples for each class would be affected.

(2) For the three existing 30m global land cover products (Globeland30, FROM_GLC, and GLC_FCS30), the classification system used for FROM_GLC level-1 has the same land cover classes used in the Globeland30, while the GLC_FCS30 has differences with others in the classification scheme and definition of land cover classes due to the inheritance from the CCI-LC classification system(Gao et al., 2020; Liu et al., 2021). As we adopted the same classification scheme as Globeland30, it was reasonable to choose the FROM_GLC rather than GLC_FCS30.

Considering both the data time and classification system, the FROM_GLC was used in our study. Given that there are inevitably errors in samples generated from the FROM_GLC, the class label from the FROM_GLC was not assigned to our samples. Instead, we checked all the points according to Google Earth high-resolution images and labeled them. Through the manual interpretation, we can guarantee the global samples are accurate.

Correspondingly, the related description of generating the global point-based samples has been updated in our revised manuscript.

"The stratified random sampling depends on area ratio of LC classes from a LC product. We used the FROM_GLC as prior knowledge rather than the Globeland30 and GLC_FCS30 with two considerations: (1) the FROM_GLC has the same data time as our target map (GLC-2015) while the Globeland30 has a 5-year interval from our samples, which affects the size of samples for each LC class; (2)the 10 level-1 land cover classes of the FROM_GLC is similar to that in the classification system of the GLC-2015, while the GLC_FCS30 has differences with the GLC-2015 in the classification scheme and definition of land cover classes." (Revised manuscript, Line 210-217)

"The FROM_GLC shows low accuracy for some LC classes, especially for cropland and forest (Gao et al., 2020; Liu et al., 2021b; Zhang et al., 2021; Zhang et al., 2022). If the global samples were extracted with LC class label from the FROM_GLC, there would be inevitable errors. Therefore, the FROM_GLC was only used to determine the size and location of samples for each LC class. Instead, all the points were manually labeled according to Google Earth high-resolution images." (Revised manuscript, Line 222-226)

References:

Gao, Y., Liu, L., Zhang, X., Chen, X., Mi, J., and Xie, S.: Consistency Analysis and Accuracy Assessment of Three Global 30-m Land-Cover Products over the European Union using the LUCAS Dataset, Remote Sen., 12, 3479, https://doi.org/10.3390/rs12213479, 2020.

Liu, L., Zhang, X., Gao, Y., Chen, X., Shuai, X., and Mi, J.: Finer-resolution mapping of global land cover: Recent developments, consistency analysis, and prospects, Journal of Remote Sensing, 5289697, https://doi.org/10.34133/2021/5289697, 2021.

Zhang, X., Liu, L., Chen, X., Gao, Y., Xie, S., and Mi, J.: GLC_FCS30: global land-cover product with fine classification system at 30 m using time-series Landsat imagery, Earth Syst. Sci. Data, 13, 2753-2776, https://doi.org/10.5194/essd-13-2753-2021, 2021.

Zhang, C., Dong, J., and Ge, Q.: Quantifying the accuracies of six 30-m cropland datasets over China: A comparison and evaluation analysis, Comput. Electron. Agric., 197, 106946, https://doi.org/10.1016/j.compag.2022.106946, 2022.

Comment #2-7. Page 198: Why select these 1507 samples randomly? Can they be determined according to their ecoregions or cover types? It is better to explain it here clearly.

Response: Thanks for the comment. It is a widely-used strategy to divide the study area into sub-regions for the large-scale or global land cover mapping. In previous work, the size of a sub-region ranged from 1°×1° to 10º×10° (Gong et al., 2020; Liu et al., 2020; Huang et al., 2021; Jin et al., 2022; Zhang et al., 2021; Zhao et al., 2021). Considering the limited memory resource on GEE and the sufficiency for land cover classes, the global land was split to 4°×4° grids. In total, there were 1507 grids across the globe.

We suspect that the reviewer is asking why we select 93 grids from a total of 1507 grids. Deriving samples according to ecoregions or cover types is suitable to increase the size of rare classes (Olofsson et al., 2014). While simple random sampling is easy to perform and capable to increase the sample size from targeted areas (Pengra et al., 2020). In our study, the patch-based samples focused more on assessing the mapping performance of our GLC-2015 map in the heterogenous landscape, such as fragmented areas and transition zones. In our previous manuscript, we just used simple random sampling to selected 93 grids and derive 5 km × 5 km patch-based samples from those grids. Then, a manual adjustment was applied to slightly increased the sample size for areas with disagreement which exists in the previous GLC maps. In this way, the sample set was more capable to verify whether the GLC-2015 improved in regions where land cover was poorly mapped by previous maps. Considering that the previous 144 patch-based samples may not enough for each ecoregion, we have added another 57 samples in the revised manuscript.

We have updated the description of collecting global path-based samples in the manuscript as follows:

"Simple random sampling was used to derive 5 km × 5 km blocks over the world's terrestrial areas because it is easy to perform and capable to augment the sample size from target areas (Pengra et al., 2020). Since inconsistency between current GLC maps tends to appear in those heterogeneous areas, such as fragmented regions and transition zones, we slightly increased the sample size for areas with the heterogeneous landscape to better evaluate our mapping results. In total, there were 201 blocks selected as the global patch-based samples, as displayed in Figure. 3a.

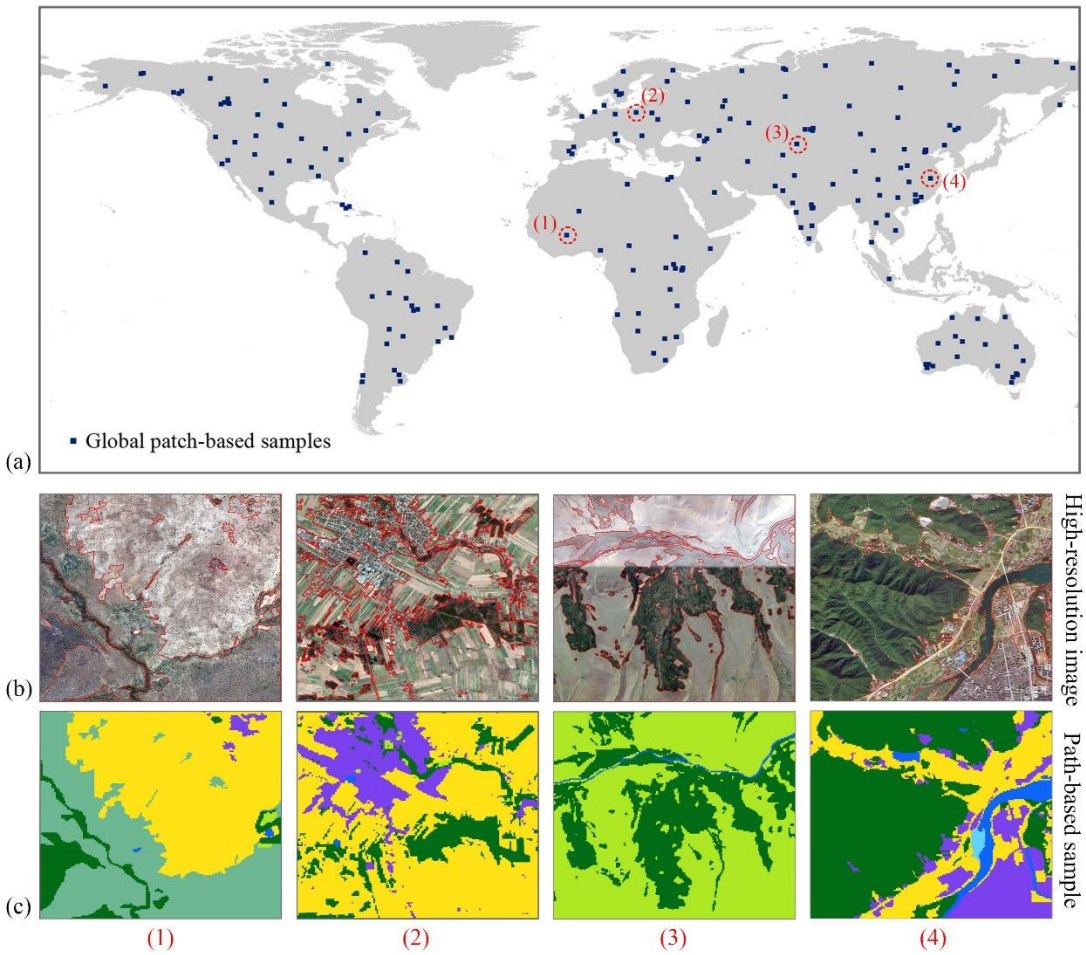

Figure 3. Spatial distribution and selected examples of the global patch-based samples. The locations of 5 km × 5 km patch-based samples are shown as panel (a), the locations of four selected samples are remarked by red dash circles. Panels (b) and (c) illustrate the production of global patch-based samples on manual interpretation. The red lines in high-resolution images circa 2015 are results after vectorization using ArcGIS 10.5 software. Four corresponding patch-based samples are shown as (c)." (Revised manuscript, Line 237-252)

References:

Gong, P., Li, X., Wang, J., Bai, Y., Chen, B., Hu, T., Liu, X., Xu, B., Yang, J., Zhang, W., and Zhou, Y.: Annual maps of global artificial impervious area (GAIA) between 1985 and 2018, Remote Sens. Environ., 236, 111510, https://doi.org/10.1016/j.rse.2019.111510, 2020.

Huang, X., Li, J., Yang, J., Zhang, Z., Li, D., and Liu, X.: 30m global impervious surface area dynamics and urban expansion pattern observed by Landsat satellites: From 1972 to 2019., Sci. China Earth Sci, 64, 1922–1933, https://doi.org/10.1007/s11430-020-9797-9, 2021.

Jin, Q.; Xu, E.; and Zhang, X.: A fusion method for multisource land cover products based on superpixels and statistical extraction for enhancing resolution and improving accuracy, Remote Sens, 14, 1676, https://doi.org/10.3390/rs14071676, 2022.

Liu, X., Huang, Y., Xu, X., Li, X., Li, X., Ciais, P., Lin, P., Gong, K., Ziegler, A. D., Chen, A., Gong, P., Chen, J., Hu, G., Chen, Y., Wang, S., Wu, Q., Huang, K., Estes, L., and Zeng, Z.: High-

spatiotemporal-resolution mapping of global urban change from 1985 to 2015, Nature Sustainability, 3, 564-570, https://doi.org/10.1038/s41893-020-0521-x, 2020.

Olofsson, P., Foody, G. M., Herold, M., Stehman, S. V., Woodcock, C.E., and Wulder, M. A. : Good practices for estimating area and assessing accuracy of land change, Remote Sens. Environ., 148, 42-57, https://doi.org/10.1016/j.rse.2014.02.015, 2014.

Pengra, B. W., Stehman, S. V., Horton, J. A., Dockter, D. J., Schroeder, T. A., Yang, Z., Cohen, W. B., Healey, S. P., and Loveland, T. R.: Quality control and assessment of interpreter consistency of annual land cover reference data in an operational national monitoring program, Remote Sens. Environ., 238, 111261, https://doi.org/10.1016/j.rse.2019.111261, 2020.

Zhang, X., Liu, L., Chen, X., Gao, Y., Xie, S., and Mi, J.: GLC_FCS30: global land-cover product with fine classification system at 30 m using time-series Landsat imagery, Earth Syst. Sci. Data, 13, 2753-2776, https://doi.org/10.5194/essd-13-2753-2021, 2021.

Zhao, J., Yu, L., Liu, H., Huang, H., Wang, J., and Gong, P.: Towards an open and synergistic framework for mappingglobal land cover, PeerJ, 9, e11877, https://doi.org/10.7717/peerj.11877, 2021.

Comment #2-8. Figure. 3 and Figure.4 can be combined.

Response: Thanks for the suggestion. Figure. 3 and Figure.4 have been combined as suggested in the revised manuscript. Moreover, we added 57 patch-based samples over the globe and three examples of the production of patch-based samples on manual interpretation. The improved figure is shown as below.

“

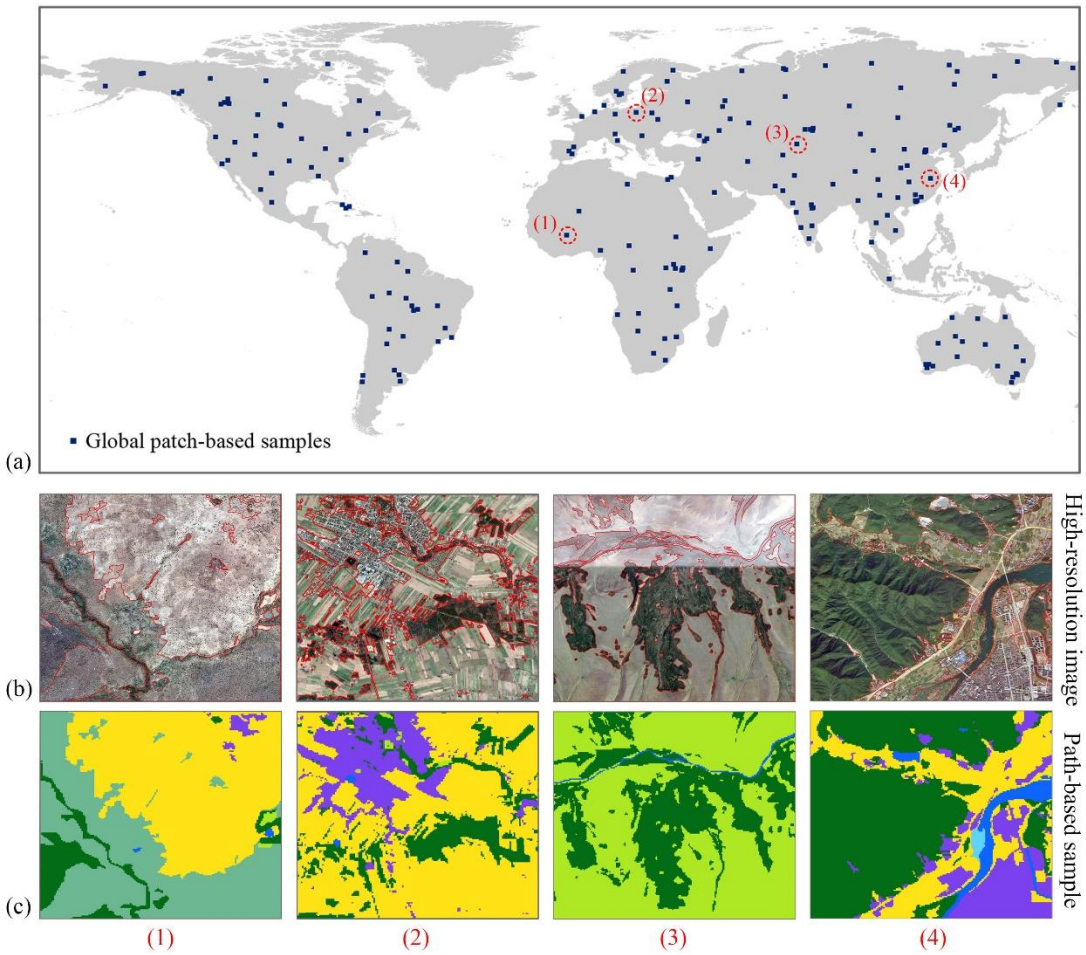

Figure 3. Spatial distribution and selected examples of the global patch-based samples. The locations of 5 km × 5 km patch-based samples are shown as panel (a), the locations of four selected samples are remarked by red dash circles. Panels (b) and (c) illustrate the production of global patch-based samples on manual interpretation. The red lines in high-resolution images circa 2015 are results after vectorization using ArcGIS 10.5 software. Four corresponding patch-based samples are shown as (c)." (Revised manuscript, Line 247-252)

Also, the main text uses "Figure" whereas the figure caption uses "Figure". Please make them consistent.

Response: Thanks for the suggestion. We have changed the "Fig" in main text as "Figure".

Comment #2-9. Page 281: how to determine these two thresholds: 25% and 75% in Eq. (4). Please explain.

Response: Thanks for the comment. We used the local adaptive fusion model to combine the existing products for each grid. To avoid the inequacy in the size of local samples for rare land cover classes, we also used global samples to evaluate products' reliability. Since the local samples plays a more critical role in the local accuracy assessment, higher weight should be assigned to the local samples in the construction of the BPA for each grid. Through the tests in several girds, it was found that when the local

samples counted for 75% of the whole sample set and the global samples counts for 25%, the fusion method exhibited robust performance and achieved relatively high accuracy. We have explained why we used 75% and 25% as two thresholds in our manuscript.

"Given that the local accuracy for a 4º×4° grid was not able to adequately reflect the actual land cover landscape, especially for the rare LC classes, global accuracy was incorporated into the construction of the BPA to avoid uncertainties from a local point of view. Since assessment based on local samples plays a more critical role in BPA construction for a local grid, higher weight should be assigned to local accuracy. In this case, we chose 75% as the weight for local accuracy and 25% for global accuracy as this ratio could achieve robust performance for different regions." (Revised manuscript, Line 331-337)